

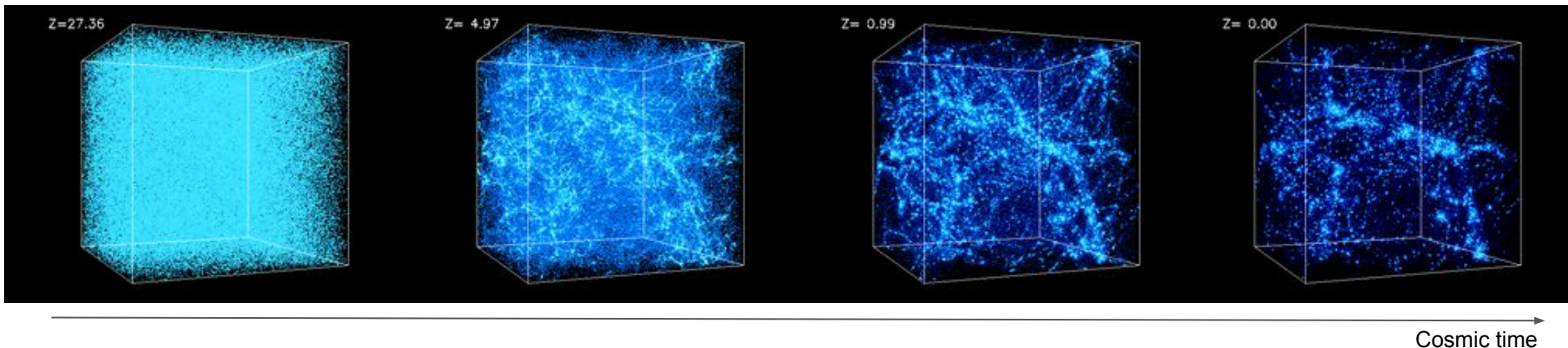
# Cluster Number Counts as a Cosmological Probe

Theory, Modelling, Simulation Inputs

work with Sebastian Bocquet, I-non Chiu, Vittorio Ghirardini, Joe Mohr,  
Matthias Klein, Tim Schrabback, Alex Saro, Matteo Costanzi,  
and the SPT, DES and eROSITA Cluster working groups

# Physical Background

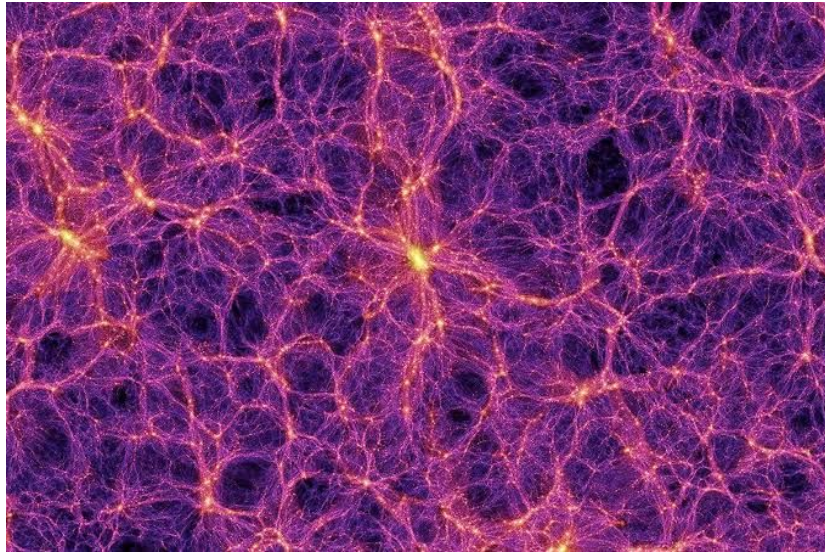
simulations were performed at the [National Center for Supercomputer Applications](#) by [Andrey Kravtsov \(The University of Chicago\)](#) and [Anatoly Klypin \(New Mexico State University\)](#). Visualizations by [Andrey Kravtsov](#).



- initial density field is homogeneous with small fluctuations
- such a configuration is gravitationally unstable  $\rightarrow$  over-density become more dense / contract, under-densities become less dense / expand  $\rightarrow$  Cosmic Web
- tracing its dynamics is a multi-scale problem  $\rightarrow$  can be solved in absence of pressure terms: collisionless fluid, drag term (expansion), Poisson equation
- $\rightarrow$  gravity-only simulations

Newton Principia, Jeans 1902, Lifshitz 47, Zeldovich 67

# Halo Formation



The densest regions of the cosmic web form *Halos*

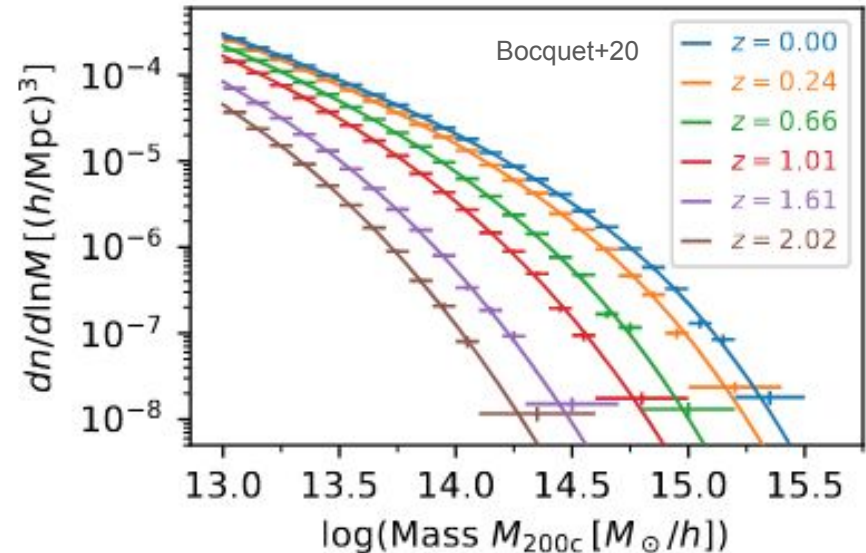
- region exceeds a given density contrast
- decouples from the background expansion
- undergoes gravitational collapse until virialization

End-result: a virialized, on average spherical ensemble of bound matter, ca. 200 times as dense as the background

Number density of halos as function of mass and redshift → *halo mass function*

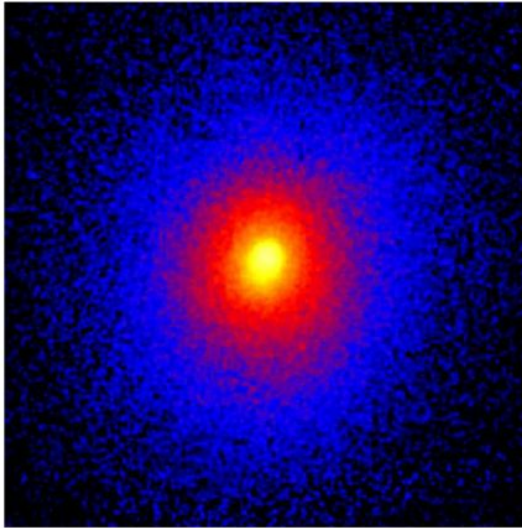
- to 0th order: fraction of density fluctuations at Lagrangian radius assoc. to the resp. mass that exceeded the density contrast
- cosmological dependent corrections (needs to be calibrated)

Tinker+08, Despali+16, Castro+21

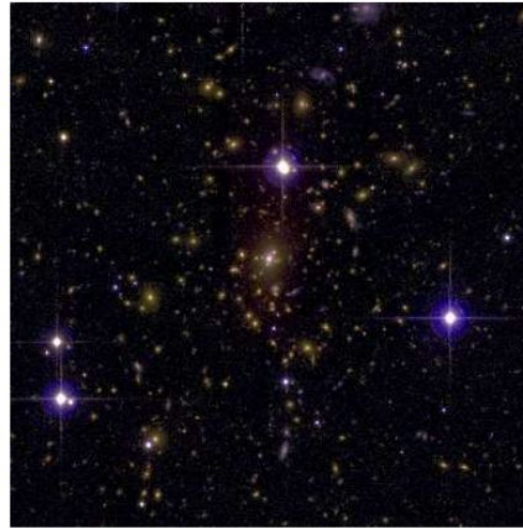


# Galaxy Clusters

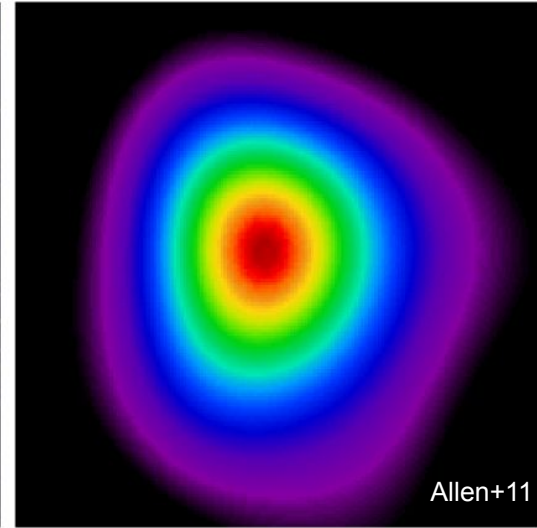
The most massive halos ( $M > 10^{14} M_{\odot}$ ) are inhabited by hot ( $T > 1$  keV) extended gas  
 → *Galaxy Clusters* observational features dominated by gravitational potential



Extended Bremsstrahlung  
 emission in X-rays



Overdensity of red galaxies  
 + massive central galaxy  
 with stellar envelope



Spectral distortion in  
 (sub-)millimeter wavelength  
 (Sunyaev-Zel'dovich effect)

# Galaxy Clusters

Galaxy clusters have an inherently multi-wavelength signature

→ reliable selection of galaxy cluster samples relies on multi-wavelength approach

## Selection of galaxy clusters

- candidate list of extended X-ray sources or “shadows” in the CMB
- optical follow-up with deep & wide optical & NIR photometry

Bleem+15/20, Hilton+21, Klein+21

Strong physical motivation for presence of massive halo:

- unique signature of hot extended gas
- coinciding with over-density of red galaxies

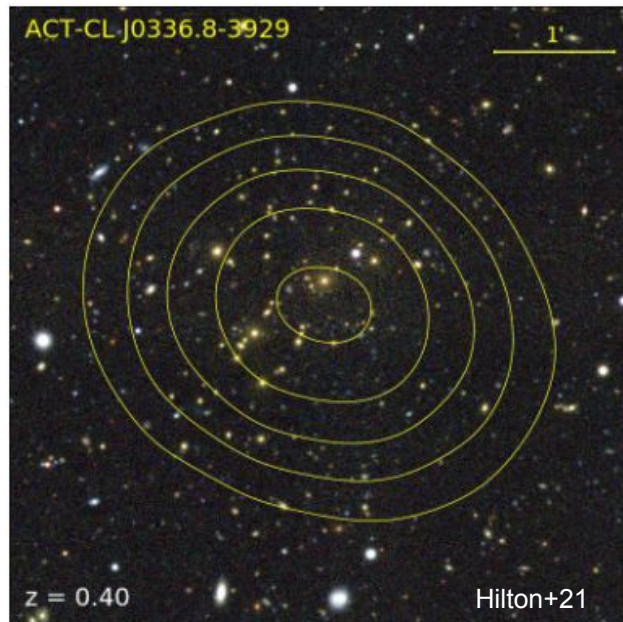
## Resulting catalog:

- two selection observables (X-ray/SZ + optical richness)
- photometric redshift with sub percent accuracy

Multi-observable cuts help empirically control  
contamination fraction

Bleem+20, SG+20, Hilton+21, Klein+21

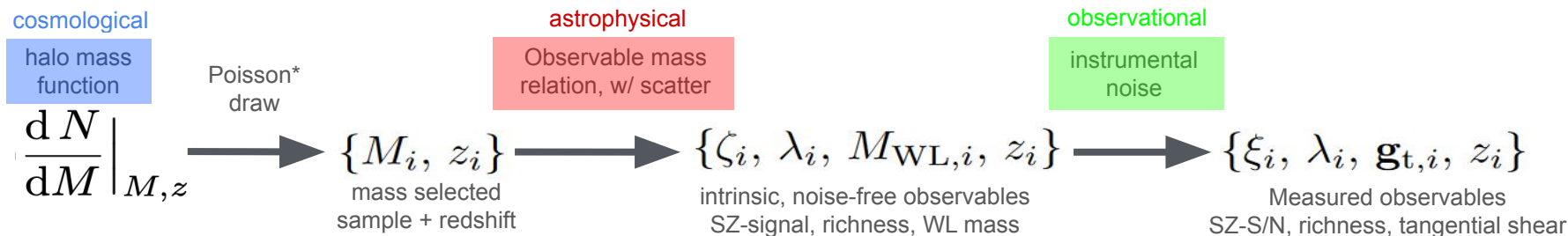
Multi Wavelength also makes pure optical selection viable, see Costanzi+21, SG+21



# Bayesian Population Modelling

- Bayesian approach: – postulate a stochastic model with free parameters that **generates** your data  
 – evaluate prop. density func. of the **actual** data as function of model parameters (*likelihood function*)

How to generate a cluster sample



Resulting multi-observable number density

reading direction

$$\frac{d^4 N(\mathbf{p})}{d\xi d\lambda d\mathbf{g}_t dz} = \int \cdots \int d\Omega_s dM d\zeta dM_{WL} P(\mathbf{g}_t | M_{WL}, \mathbf{p}) P(\xi | \zeta) P(\zeta, \lambda, M_{WL} | M, z, \mathbf{p}) \frac{d^3 N(\mathbf{p})}{dM dz dV} \frac{dV(z, \mathbf{p})}{d\Omega_s}$$

marginalizes over  
latent variables

More things can be added: sky position dependence, errors on richness, more observables

Likelihood Function: Data generating process is a Poisson Process

Working on addition of sample variance following Lacasa&Grain19

Poisson Distribution of  $k$  observed events for  $\mu$  expected events

$$P(k|\mu) = \frac{\mu^k e^{-\mu}}{k!} \Rightarrow \ln P(k|\mu) = k \ln \mu - \mu + \text{const.}$$

For fine bins in observable space (s.t. each bin contains one cluster  $i$ )

$$\ln \mathcal{L} = \sum_i \ln \mu_i - \sum_j \mu_j \quad \text{Following Mantz+15}$$

Limit of infinitesimally small bins

$$\ln \mathcal{L}(\mathbf{p}) = \sum_i \ln \left. \frac{d^4 N(\mathbf{p})}{d\xi d\lambda d\mathbf{g}_t dz} \right|_{\xi_i, \lambda_i, \mathbf{g}_{t,i}, z_i} - \int \dots \int d\xi d\lambda d\mathbf{g}_t dz \frac{d^4 N(\mathbf{p})}{d\xi d\lambda d\mathbf{g}_t dz} \Theta_s(\xi, \lambda, z) \quad \text{Selection cuts}$$

This sum runs over selected clusters, so they fulfill the selection cuts

Free model parameters: – cosmological parameters (for HMF, and cosmo dep of observables)  
– observable mass scaling relation parameters, scatters and correlation coefficients (see below)

# Observable Mass Relations

Strong physical prior:

Galaxy cluster are gravity dominated objects

Scaling relation are power laws, and close-ish to self-similar scaling

Allow for unknown:

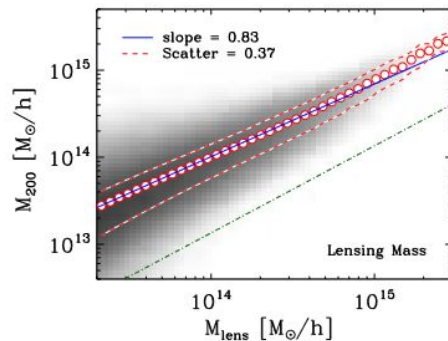
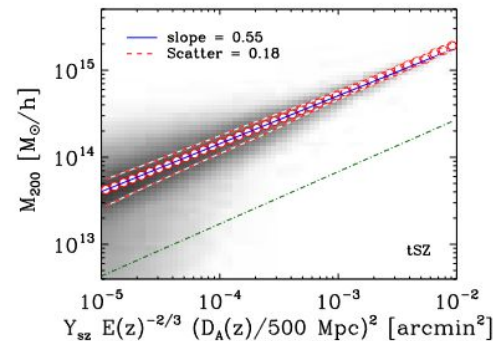
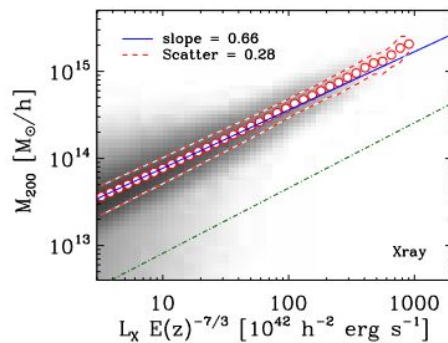
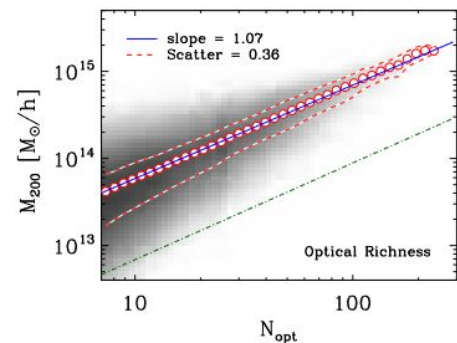
Amplitude, mass trend, deviation from self-similar redshift trend

In this way, the X-ray observable-to-mass-and-redshift ( $\mathcal{X} - M_{500-z}$ ) relation reads,

$$\langle \ln \mathcal{X} | M_{500} \rangle = \ln A_{\mathcal{X}} + \left[ B_{\mathcal{X}} + \delta_{\mathcal{X}} \ln \left( \frac{1+z}{1+z_{\text{piv}}} \right) \right] \times \ln \left( \frac{M_{500}}{M_{\text{piv}}} \right) + C_{\text{SS},\mathcal{X}} \times \ln \left( \frac{E(z)}{E(z_{\text{piv}})} \right) + \gamma_{\mathcal{X}} \times \ln \left( \frac{1+z}{1+z_{\text{piv}}} \right), \quad (46)$$

with log-normal intrinsic scatter at fixed mass of

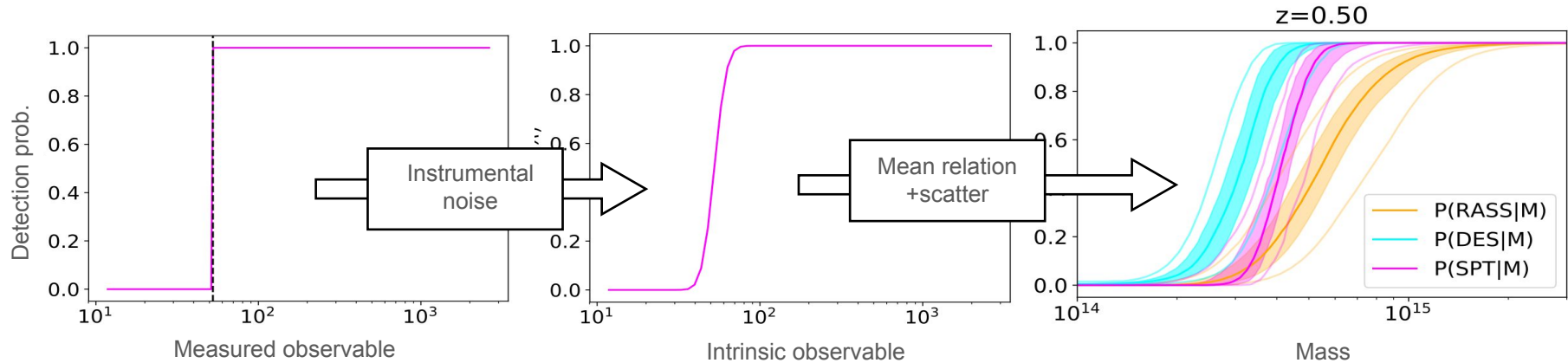
$$\sigma_{\mathcal{X}} \equiv (\text{Var} [\ln \mathcal{X} | M_{500}])^{\frac{1}{2}}, \quad \text{As presented in Chiu+22, but wild variety of notations can be found} \quad (47)$$



# The Role of observable scatter

Mean scaling between observable and mass + its scatter directly predict incompleteness as function of mass  
A.k.a “Selection Function”

This model, the selection function is constructed semi-analytically  
JBM presented similar thoughts at Euclid Cluster meeting in Bologna



Clusters are selected by imposing a cut in the selection observable(s)

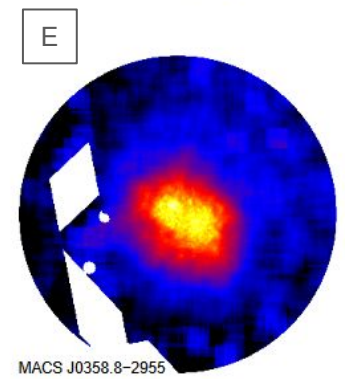
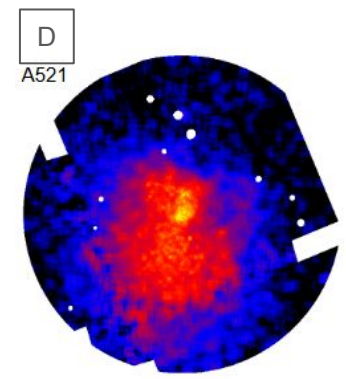
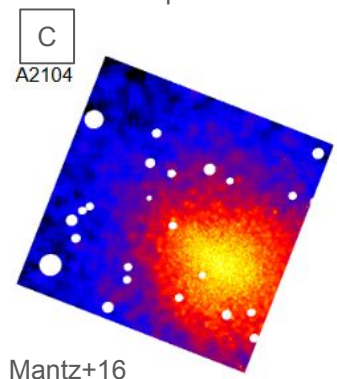
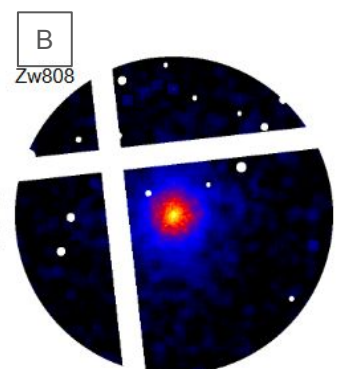
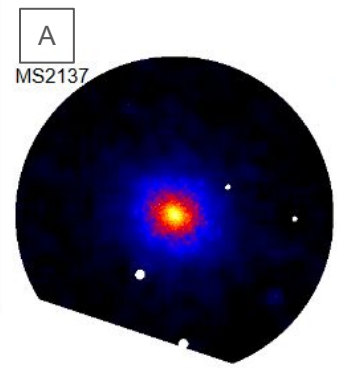
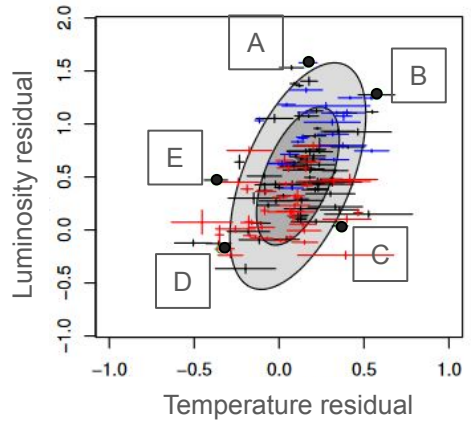
Applying scatter sources and mean observable mass relation gives the mass incompleteness  
Crucially with systematic uncertainty!!

Need to empirically constrain the mean relation between selection observable and halo mass

Image simulation used only to understand instrumental noise effects

# The true nature of “selection bias”

At fixed mass, the intrinsic scatters of different observable might correlate due to joint physical causes for their deviation from the mean relation → introduce *correlation coefficients* among them



Eddington bias: Any sample has preferentially objects that scatter up in selection observable  
Given that there are many more low mass than high mass objects

Propagation to other observables Wu+22

$$\langle \ln \Sigma | \ln \lambda, M \rangle = \langle \ln \Sigma | M \rangle + r \sigma_{\ln \Sigma} \frac{(\ln \lambda - \langle \ln \lambda | M \rangle)}{\sigma_{\ln \lambda}}$$

Correlation coefficient

Sigmas of Eddington bias

→ correlation coefficients as free parameters

# Mass calibration

Lets count the number of free parameters if we have  $N$  observables

And see if the data can constrain them

We only have  $N-1$  observable–observable scatter plots

→ can constrain  $N-1$  relations

→ inference problem is underdetermined

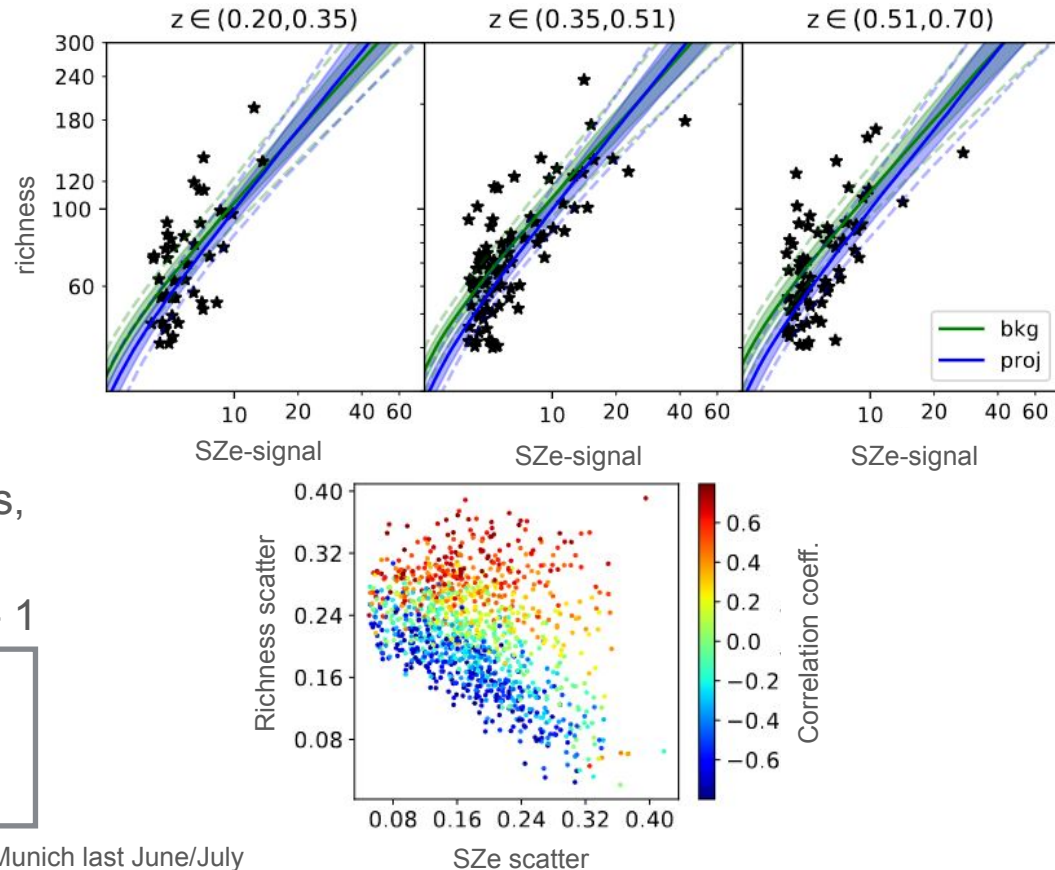
→ need external priors on one observable mass relation

→ no problem for scatter parameters: we measure obs–obs scatter for upper bounds, and lower bound is 0

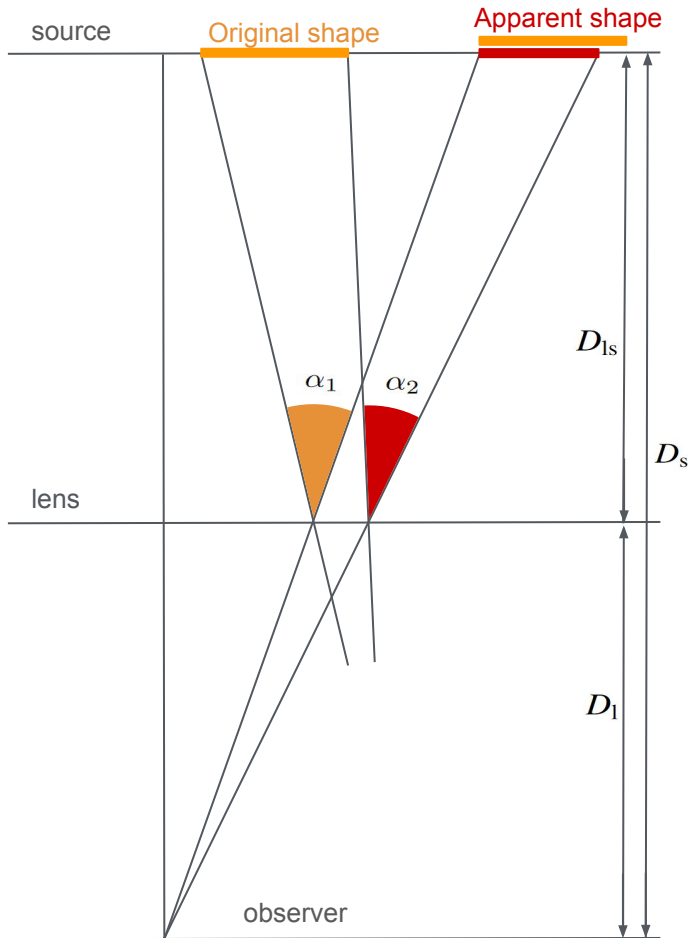
→ correlation coefficients are bound by  $\pm 1$

Weak gravitational lensing as anchor, as it has the least baryonic modelling uncertainties

Not sure how made this point first, AvdL made it quite clearly in Munich last June/July



# WL by massive halos



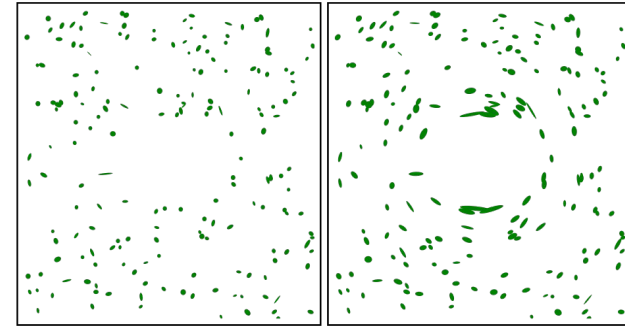
Gravitational potentials bend space time, and therefore *deflect light*,  $\vec{\alpha} = -\vec{\nabla}\phi$

Differential deflection,  $\alpha_2 < \alpha_1$ , leads to a *tangential distortion* of background images

Background source are on average round, hence averaging many such sources reveals the coherent tangential distortion

The strength of the distortion is modulated by the geometrical configuration

$$\Sigma_{\text{crit,ls}}^{-1} = \frac{4\pi G}{c^2} \frac{D_l}{D_s} \max[0, D_{ls}]$$



Source: Wikipedia

Sources: galaxies from wide photometric survey with shape and photo-z measurement (DES, HSC, KiDS)

Optimal mass extraction results from fitting shear profile with shear profile model

Gruen+11, fitting shear profiles > any aperture mass

The mass that results from fitting a shear profiles with a model is called *weak lensing mass*

Becker+Kravtsov 11

It is biased w.r.t. and scatters around the true halo mass

→ *WL bias and scatter*

Mass anchor consists in reliable WL bias and scatter priors, than represent the *mass accuracy*

Applegate+14, Dietrich+19

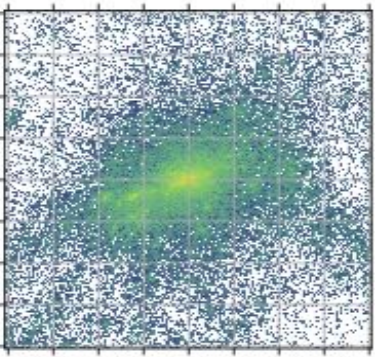
## Challenges and Solutions for <1% accuracy

Castro+21

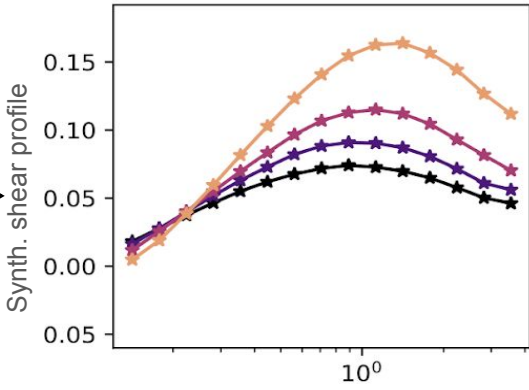
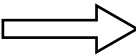
- hydrodynamical effects don't destroy halos, HMF are calibrated on gravity only → calibrate WL mass vs gravity only halo mass
  - shape noise only dictates radial weighting in extraction → work in limit of no shape noise + area weighting
  - need dedicated simulation output: fine (10 kpc pixels) 2d mass map, 6 Mpc/h from center, projected for >20 Mpc along LoS
    - work on particle data
  - mis-center first, then compute tangential shear with Kaiser-Squires
  - compute reduced shear at map level, and for each source plane, then average
- Learned after 21 :D

# Computing the mass anchor

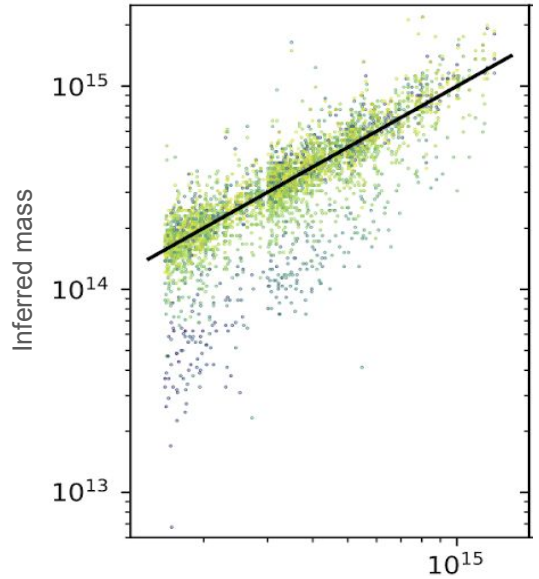
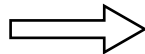
Matter distribution around halos



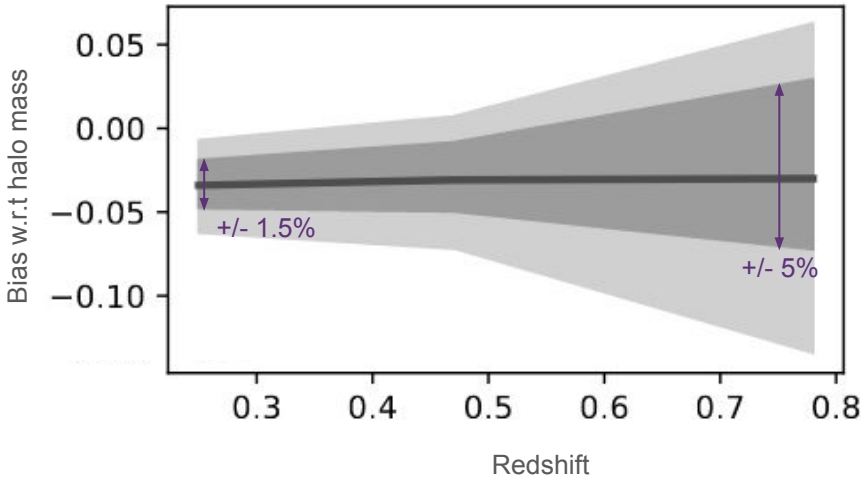
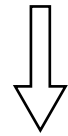
From hydro simulations



Cluster centric distance

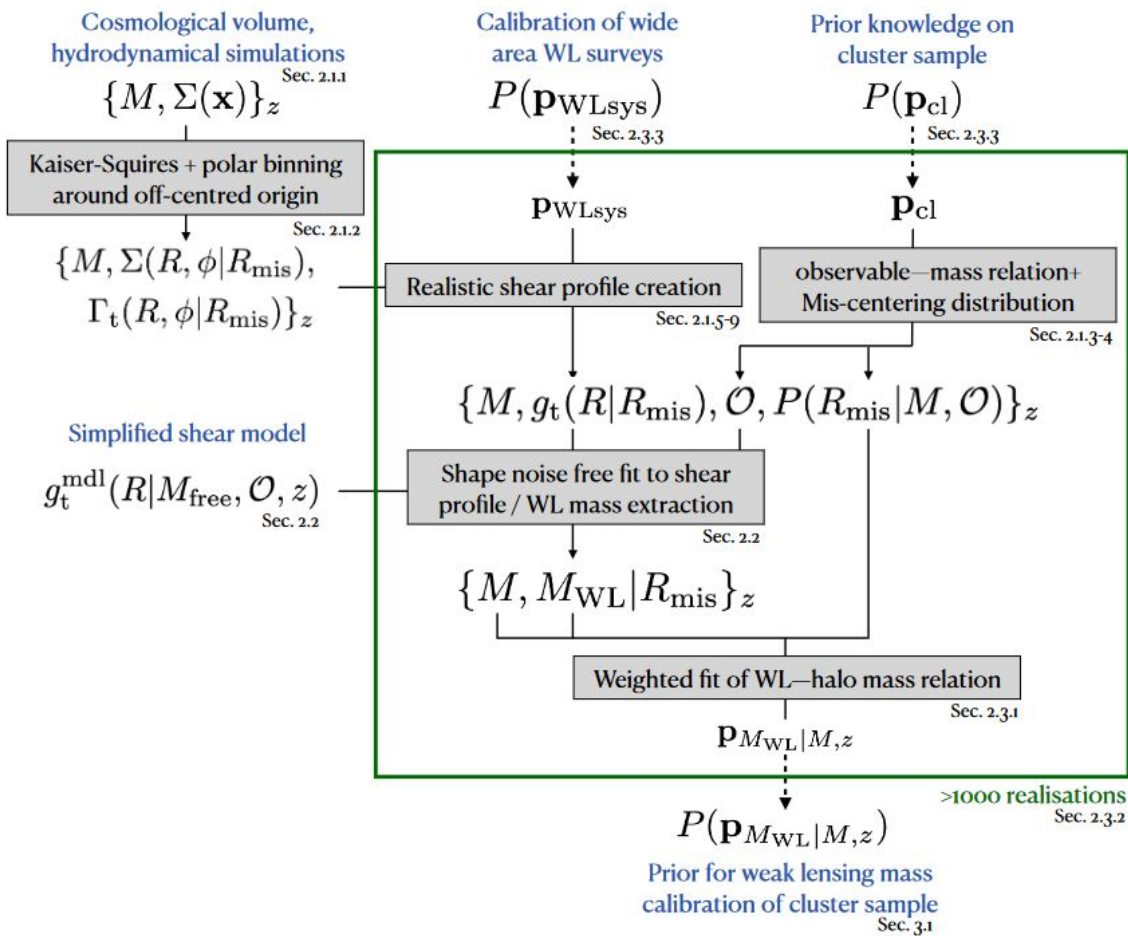


Input mass



WL mass bias with error estimate  
from Monte Carlo realisations

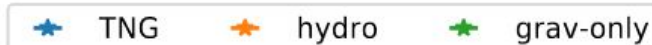
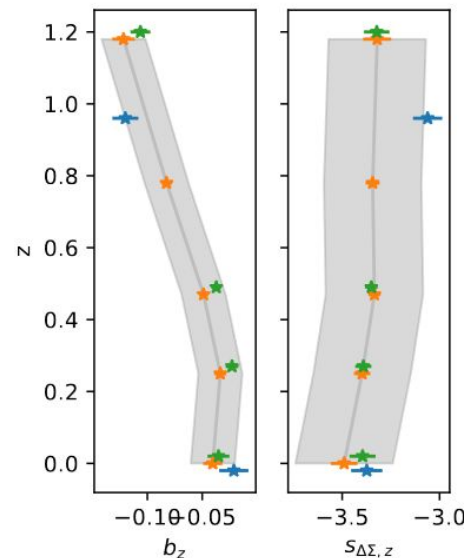
# Computing the mass anchor



Full flow chart with Monte Carlo marginalisation

Changing between Magneticum and Illustris-TNG changes the WL bias by 0.02

In optimal setting  $R_{\text{min}}=0.5 \text{ Mpc}/h$



# Practical Results

## eROSITA Equatorial Field + HSC WL

$$\langle \ln(b_{\text{WL}}|M, z) \rangle = \ln A_{\text{WL}} +$$

Chiu+22,23

$$B_{\text{WL}} \times \ln\left(\frac{M}{2 \times 10^{14} h^{-1} M_{\odot}}\right) + \gamma_{\text{WL}} \times \ln\left(\frac{1+z}{1+0.6}\right), \quad (26)$$

with log-normal intrinsic scatter  $\sigma_{\text{WL}}$  at fixed mass and redshift,

$$\sigma_{\text{WL}} \equiv (\text{Var}[\ln(b_{\text{WL}}|M, z)])^{\frac{1}{2}}.$$

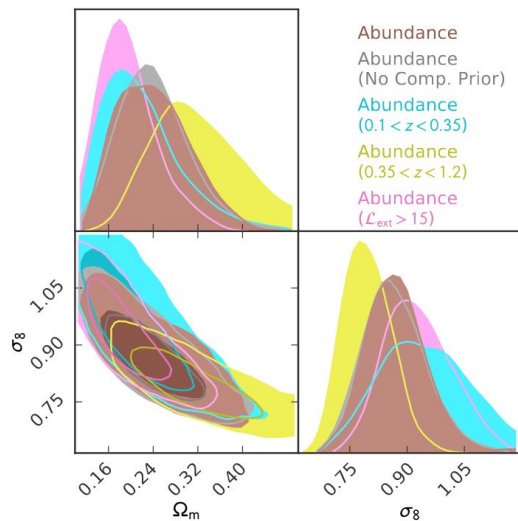
(27)

$$A_{\text{WL}} = 0.903 \pm 0.030,$$

$$B_{\text{WL}} = -0.057 \pm 0.022,$$

$$\gamma_{\text{WL}} = -0.474 \pm 0.062,$$

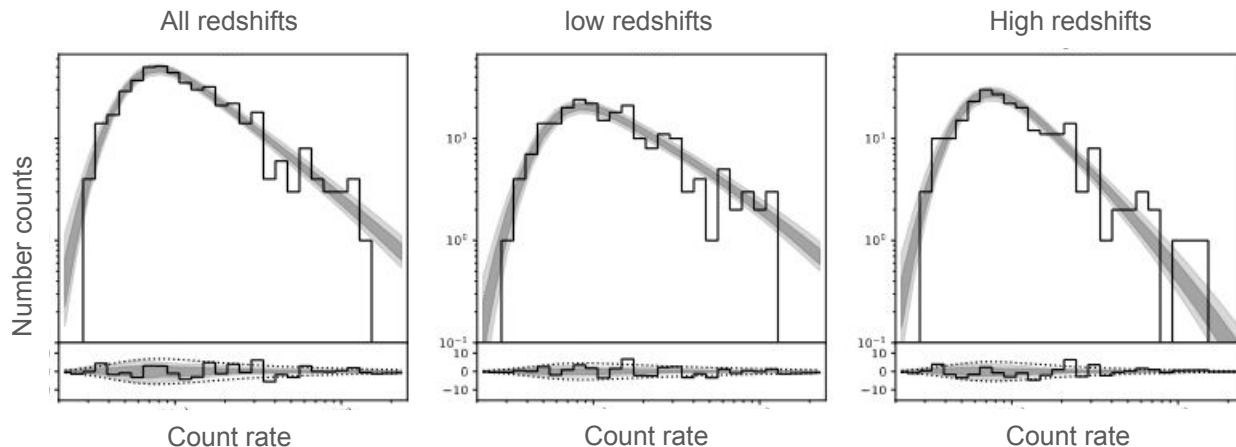
$$\sigma_{\text{WL}} = 0.238 \pm 0.037,$$



Cosmological constraint

$$S_8 \equiv \sigma_8 (\Omega_m/0.3)^{0.3} = 0.791^{+0.028}_{-0.031}$$

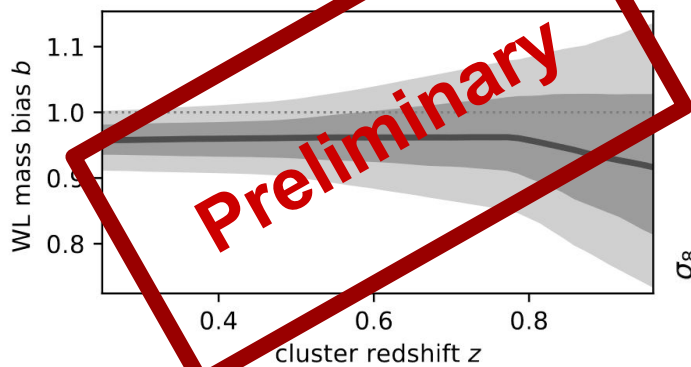
Stable against ignorance of X-ray incompleteness



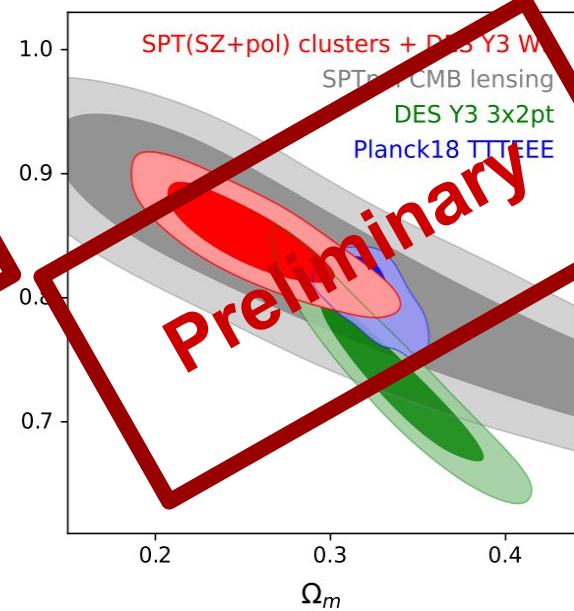
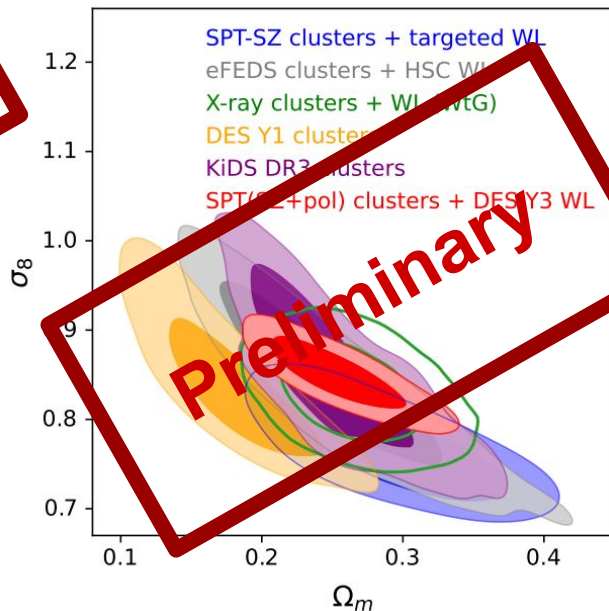
- Redshift dependent downturn in number counts as function of count rate
- unique feature, can only be explained by X-ray incompleteness
- fitting for it does not significantly deteriorate cosmological constraints

# Practical Results

SPT-(SZ+pol) + (DES Y3 + HST) WL Bocquet+ip, just unblinded



Only quantitative hydro input are  
surface mass density maps for  
WL anchoring!!



$\Omega_m$

$\sigma_8$

S8

S8opt

$0.254 \pm 0.032$

$0.850 \pm 0.026$

$0.779 \pm 0.031$

$0.835 \pm 0.015$

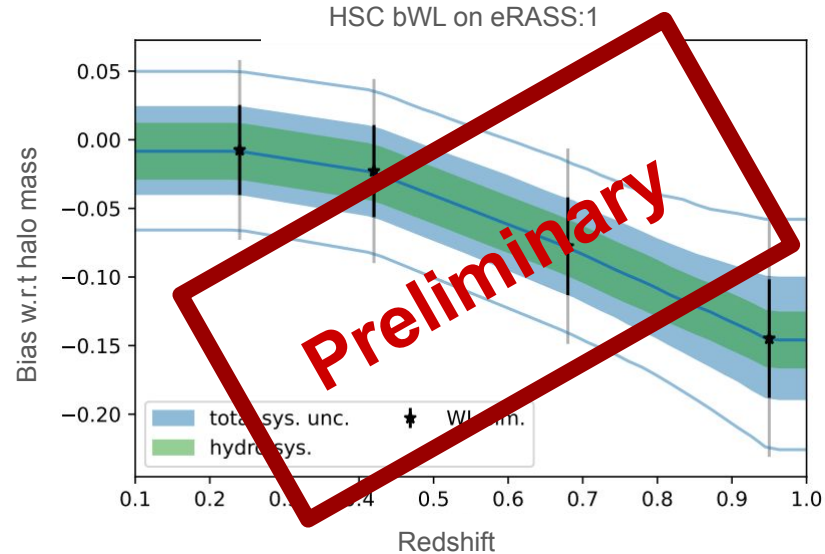
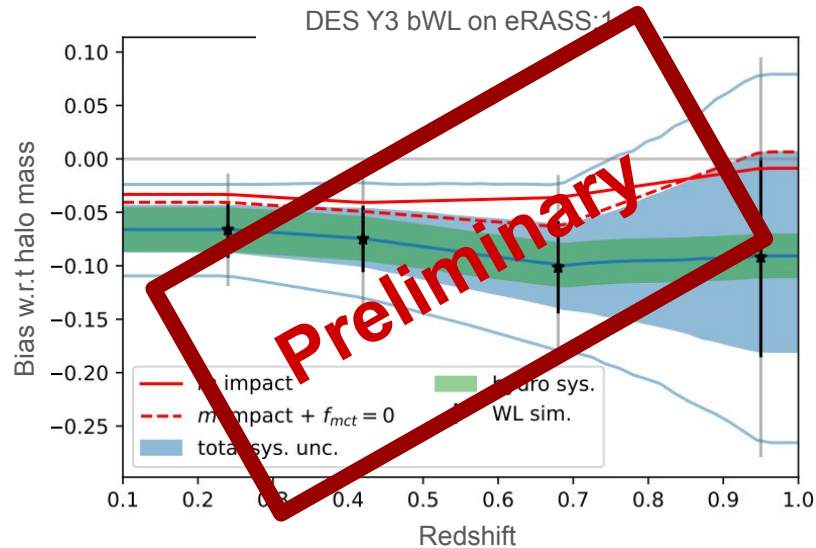
Same degeneracy direction as CMB lensing,  
ACT CMB lensing, Frank+23

$$S_8^{\text{CMBL}} \equiv \sigma_8 (\Omega_m/0.3)^{0.25}$$

$$S_8^{\text{CMBL}} = 0.818 \pm 0.022$$

# Setting the Stage for Stage IV

- Deep optical and NIR will settle current optical confirmation difficulties at  $z > 1$
  - current WL systematics: DES Y3 photo-zs dominate  $z < 0.4$ , irrelevant below. Driven by bad background selection in DES
- HSC shape uncertainty still of same order of magnitude as hydro-systematics



Working assumption for Stage IV: DES photo-z accuracy to  $z > 1$  (like HSC) + better shape measurements than HSC → we are left with 2% floor from comparison of hydro sims...

# Conclusions

## Key Ingredients:

- physically motivated, multiwavelength selection to get clean cluster sample
- agnostic Bayesian population model – weak lensing measurements – grav. only HMF
- anchoring of weak lensing mass (here we bridge the gap between hydro and gravity only)

Unproven hunch: hydro impact on 2d projected density contrast weaker than on 3d halo mass...

Most pressing practical issue: – how improve hydro accuracy on WL mass to 1%  
(data constrained hydro sims?)

## Surprising Facts about WL calibrated number counts

- No need for a dedicated “selection function”, can be fitted on the fly without cosmology loss
- already in Stage III surveys, hydrodynamics floor is limiting factor (at low  $z$ )
- thanks to strong (qualitative) physics prior far less susceptible to baryon physics than cosmic shear and galaxy correlations (baryonic effects on power spectrum, intrinsic alignment, non-linear bias, assembly bias, non linear power spectrum, ...)
- “S8 tension” not confirmed (likely modelling issues in cosmic shear cross galaxies)